AGU PUBLICATIONS

JGR

Journal of Geophysical Research: Oceans

RESEARCH ARTICLE

10.1002/2016JC012549

Biological and physical controls on the flux and characteristics of sinking particles on the Northwest Atlantic margin

Jeomshik Hwang[1,2], Steven J. Manganini[2], JongJin Park[3], Daniel B. Montluçon[2,4], John M. Toole[2], and Timothy I. Eglinton[2,4]

[1]School of Earth and Environmental Sciences/Research Institute of Oceanography, Seoul National University, Seoul, South Korea, [2]Woods Hole Oceanographic Institution, Woods Hole, Massachusetts, USA, [3]Department of Oceanography, Kyungpook National University, Daegu, South Korea, [4]ETH Zürich, Zürich, Switzerland

Key Points:
- POC and opal fluxes to NW Atlantic margin deep waters are mainly controlled by biological production in surface waters
- $CaCO_3$ and lithogenic material predominantly derive from lateral transport of resuspended sediment
- Resuspended sediment accounts for ca. 63% of the total particle flux at 3000 m

Supporting Information:
- Supporting Information S1

Correspondence to:
J. Hwang,
jeomshik@snu.ac.kr

Citation:
Hwang, J., S. J. Manganini, J. Park, D. B. Montluçon, J. M. Toole, and T. I. Eglinton (2017), Biological and physical controls on the flux and characteristics of sinking particles on the Northwest Atlantic margin, *J. Geophys. Res. Oceans*, *122*, 4539–4553, doi:10.1002/2016JC012549.

Received 14 NOV 2016
Accepted 8 MAY 2017
Accepted article online 15 MAY 2017
Published online 1 JUN 2017

Abstracts Biogenic matter characteristics and radiocarbon contents of organic carbon (OC) were examined on sinking particle samples intercepted at three nominal depths of 1000 m, 2000 m, and 3000 m (~50 m above the seafloor) during a 3 year sediment trap program on the New England slope in the Northwest Atlantic. We have sought to characterize the sources of sinking particles in the context of vertical export of biogenic particles from the overlying water column and lateral supply of resuspended sediment particles from adjacent margin sediments. High aluminum (Al) abundances and low OC radiocarbon contents indicated contributions from resuspended sediment which was greatest at 3000 m but also significant at shallower depths. The benthic source (i.e., laterally supplied resuspended sediment) of opal appears negligible based on the absence of a correlation with Al fluxes. In comparison, $CaCO_3$ fluxes at 3000 m showed a positive correlation with Al fluxes. Benthic sources accounted for 42 ~ 63% of the sinking particle flux based on radiocarbon mass balance and the relationship between Al flux and $CaCO_3$ flux. Episodic pulses of Al at 3000 m were significantly correlated with the near-bottom current at a nearby hydrographic mooring site, implying the importance of current variability in lateral particle transport. However, Al fluxes at 1000 m and 2000 m were coherent but differed from those at 3000 m, implying more than one mode of lateral supply of particles in the water column.

1. Introduction

Studies seeking to understand sinking particle flux and related biological carbon pump using time-series sediment trap moorings have been carried out at numerous locations [e.g., *Honjo et al*., 2008; *Turner*, 2015]. Many of these stations represent open ocean environments where particle flux is mainly controlled by production and export of biogenic particles from the overlying surface ocean. Moreover, studies have mostly focused on the attenuation in flux, biogenic matter degradation, and remineralization during the vertical transit of particles from surface to deep waters, as well as their sedimentation. While much remains to be understood concerning the underlying mechanisms, these studies have helped to develop the concept and advanced our understanding of the biological pump, and on its role in the ocean's ability to take up atmospheric CO_2 [*Turner*, 2015].

Continental margins account for 10–20% of marine primary production and >40% of carbon sequestration by the oceanic biological pump globally [*Hedges*, 1992; *Behrenfeld and Falkowski*, 1997; *Muller-Karger et al*., 2005]. Continental margins are energetic and dynamic environments that are influenced by tidal action as well as strong across- and/or along-shelf currents. At some locations, these along-shelf currents are strong enough to resuspend surface sediments and transport clay- and silt-sized particles [*Hollister and McCave*, 1984; *Inthorn et al*., 2006; *Karakas et al*., 2006; *McCave and Hall*, 2006; *Bao et al*., 2016]. In addition, cross-shelf currents and jets that emanate from the shelf break can entrain fine particles and transport them toward the interior of the ocean [*Pickart*, 2000; *McCave et al*., 2001]. Therefore, characteristics and trajectories of particle flux over continental margins can differ markedly from those in the open ocean.

Several previous studies have reported lateral transport of particulate organic carbon (POC) at various locations over continental margins evidenced by direct observations and indirect implications of particle properties (see references in *Hwang et al*. [2009b]). *Hollister and Nowell* [1991] provided photographic evidence

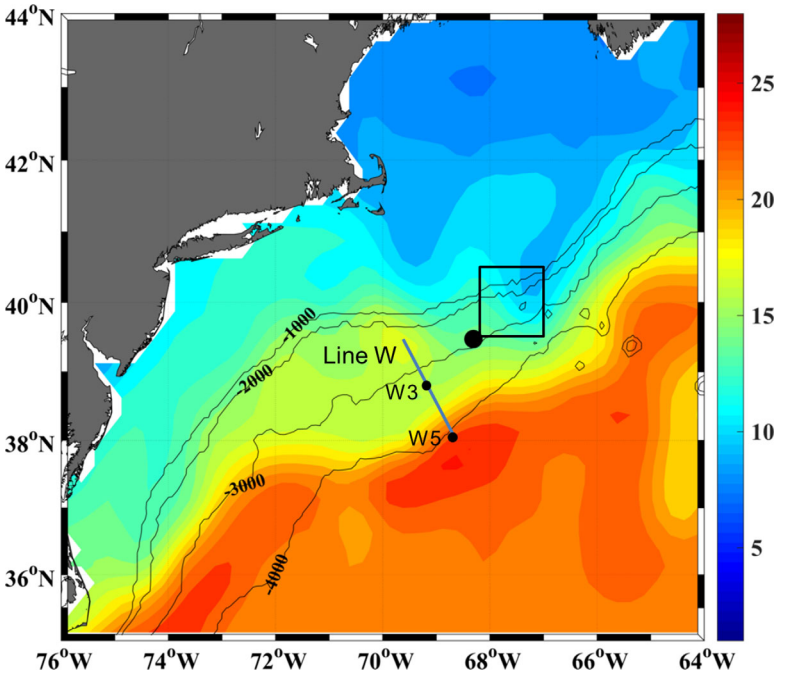

Figure 1. Satellite-derived sea surface temperature (SST) on January 1, 2005 overlain on bathymetry in the northwest Atlantic. Sediment trap mooring station (large circle) and MMP moorings (small circles) along the Line W transect are indicated. The rectangle denotes the area for which chlorophyll-*a* concentrations were obtained. This area roughly corresponds to the provenance of fresh sinking POC based on alkenone-temperature [*Hwang et al.*, 2014].

that strong currents are not confined to the shallow continental shelf but are widespread near the seafloor throughout the ocean basins (see Figure 1 in their paper). In particular, evidence for intermittent sediment-transporting events has been found for the western flank of the North and South Atlantic basin, around South Africa, and circum-Antarctic region [*Hollister and Nowell*, 1991]. Sediment mobilization inevitably also transports POC because of the tight association between high surface area mineral (clay) particles and organic matter [e.g., *Keil and Hedges*, 1993; *Mayer*, 1994]. This portion of POC is presumably aged and more refractory in nature [e.g., *Pusceddu et al.*, 2005] due to temporary storage in sediments and close association with fine-grained minerals. Resuspension of aged POC into the water column is thus likely to influence the quality of POC as food to zooplankton and other heterotrophic organisms. Characterization of the fluxes and composition of sinking particles on continental margins is necessary to better understand POC transport and burial in these productive and dynamic environments [*Muller-Karger et al.*, 2005; *Dunne et al.*, 2007; *Thunell et al.*, 2007].

We initiated a study to examine sinking and suspended particles, as well as underlying sediments in order to understand the modes and dynamics of particle transport over the New England slope on the NW Atlantic margin. This region is a dynamic environment that is influenced by the interaction of two major current systems – the Deep Western Boundary Current (DWBC) and the Gulf Stream. These are major limbs of the Meridional Overturning Circulation of the North Atlantic Ocean at midlatitude, with the Gulf Stream transporting warm water poleward and the DWBC transporting colder intermediate and deep waters southward [*Toole et al.*, 2011]. A major focus of our study was to understand the role of the DWBC as a conduit for along-margin particle transport and the source(s) of organic matter deposited in the vicinity of the DWBC, and to assess temporal variability of lateral particle transport in the context of hydrographic properties [*Hwang et al.*, 2009b]. The results from an initial 1 year study of the properties of sinking particles and suspended particles have been reported previously [*Hwang et al.*, 2009a,2009b]. The examination of the sinking particle samples collected from summer 2004 to summer 2005 strongly implied that lateral input of resuspended sediment particles was a prominent feature at this site. We found that at least two modes of lateral particle transport exist through intermediate nepheloid layers (INLs) and benthic nepheloid layers (BNLs). Supply of resuspended sediment emanating from the shelf break appears to form the INLs [*Hwang et al.*, 2009a]. In contrast, relatively brief turbidity pulses appeared to supply laterally transported particles near

the bottom [*Hwang et al*., 2009b]. Based on radiocarbon mass balance, we estimated that between 24 and 34% of sinking POC intercepted by the traps and between 15 and 54% of fine suspended POC was derived from lateral advection of resuspended shelf and/or slope sediment [*Hwang et al*., 2009a,2009b].

Building on these previous studies [*Hwang et al*., 2009a,2009b,2014] investigating the influence of lateral supply of resuspended particles on POC, here we report time-series sinking particle flux and composition data extended to 3 years, from summer 2004 to summer 2007, and examine temporal variations in the context of local hydrographic conditions. Our findings from this extended time-series data set reinforce the main observations from the initial investigation, and shed further light on the major factors controlling the observed particle fluxes and compositions. We assess results in the context of production and vertical transport of biogenic particles, and lateral input of resuspended sediment particles in relation to hydrographic conditions and the strength of the DWBC.

2. Methods

The bottom-tethered mooring was deployed at 39.5°N, 68.3°W within the core of the DWBC on the New England slope (Figure 1). Three conical sediment traps (McLane Mark-7) [*Honjo and Doherty*, 1988] were deployed at three nominal depths of 1000 m, 2000 m, and 3000 m (50 m above the seafloor) from summer 2004 to summer 2007, with hiatuses of 1–2 months due to recovery and redeployment of the moorings. Trap depths, duration, sample cup opening intervals, location, and water depth of each deployment are listed in Table 1. A SBE19 SEACAT CTD equipped with an optical backscatter sensor (Seapoint Turbidity Meter) was attached to the 3000 m trap frame during the second year deployment and yielded temperature, salinity, pressure, and turbidity data at 10 min interval.

During each deployment, 13 samples were collected from the 1000 m trap and 21 samples each from 2000 m and 3000 m traps. Sampling cups of the 1000 m and 2000 m traps of the first and second year deployments were filled with seawater treated with various preservatives such as $HgCl_2$, formalin, Lugol's solution, DMSO (dimethyl sulfoxide), and HISTOCHOICE^{TM} for the purpose of testing their relative efficiency of DNA preservation (not discussed further in this paper; see supporting information Table S1 for details [*Dennett and Manganini*, 2006]). $HgCl_2$ was used for the 3000 m trap of the first and second year deployments, and was exclusively used for the third year deployment. Upon trap recovery the cups were capped and stored in a refrigerator until processing. At Woods Hole Oceanographic Institution (WHOI), samples were separated into two size fractions, >1 mm and <1 mm, by sieving. Each sample <1 mm was divided into ten equal aliquots in either 40 ml glass vials or 50 ml polypropylene conical centrifuge tubes using a wet sample splitter (WSD-10, McLane Research Laboratories, Inc.).

Samples for elemental analysis were deposited on preweighed 25 mm or 47 mm polycarbonate filters, rinsed with ultrapure (Milli-Q) water and then air-dried at 60°C overnight. The mass of both size-fractions was determined for flux determination. For further chemical analyses, only fractions <1 mm were used. Total carbon and nitrogen contents were analyzed using a Perkin-Elmer 2400 CHN analyzer. Concentrations of elements (Al, Ca, Fe, and Si) were measured using an ICP-ES (Jobin-Yvon Horiba ULTIMA2) [*Honjo et al*., 1995]. Concentrations of lithogenic particles, biogenic opal, and $CaCO_3$ were estimated from Al, Si, and Ca concentrations [*Taylor and McLennan*, 1985; *Honjo et al*., 1995]. Briefly, the lithogenic material content was estimated under the assumption that Al was exclusively supplied by lithogenic debris (i.e., lithogenic material content $=$ Al$\times$12.15 $=$ Al/0.0823, where 0.0823 is the content of Al in the average continental crust [*Taylor*, 1964]). Opal and $CaCO_3$ was estimated from the following equations, respectively: Opal $=$ biogenic Si$\times$2.4 $=$ (total Si $-$ 3.5$\times$Al)$\times$2.4, and $CaCO_3$ $=$ biogenic Ca$\times$2.5 $=$ (total Ca $-$ 0.5$\times$Al)$\times$2.5 [*Valdes et al*.,

Table 1. Sampling Periods, Number of Samples, Time Interval of Each Sample, Trap Depths, and Water Depth for Three Deployments

	Sampling Period (mm/dd/yy)	Water Depth (m)	Actual Trap Depth (m)			1000 m Trap		2000 m and 3000 m Traps	
			1000 m	2000 m	3000 m	Sampling Interval (days)	# of Samples	Sampling Interval (days)	# of Samples
First year	06/27/04 ~ 04/27/05	2988	968	1976	2938	23.38	13	14.48	21
Second year	07/01/05 ~ 06/01/06	2980	1011	1968	2930	25.77	13	15.95	21
Third year	06/27/06 ~ 06/01/07	2961	992	1949	2911	26.08	13	16.14	21

2014]. Particulate inorganic carbon (PIC) content was estimated from the content of biogenic Ca: PIC = (total Ca − 0.5×Al)×0.3. PIC content of several selected samples from the first year deployment (n = 18) was also determined by coulometric titration using UIC Coloumetrics equipped with an acidification module CM5130. The difference of PIC contents in per cent determined by both methods was 0.2 ± 0.6 (relative difference = 2.6 ± 12%). Organic carbon content was estimated as the difference between the total carbon and PIC. Particulate organic matter was estimated to be 2.5×POC [*Thunell*, 1998]. The samples treated with DMSO and Histochoice gave unusually low values for Ca, and for Al, Si, and Ca, respectively. Hence, information of flux and concentration of each element and biogenic component on these samples was deemed unreliable (supporting information Table S1) and was not used for calculation of annual average values or any statistical analyses (shown as gaps in Figure 3). The concentration and flux of $C_{37:2}$ and $C_{37:3}$ alkenones have been published previously [*Hwang et al*., 2014].

For carbon isotope analysis, only samples treated with $HgCl_2$ or formalin were used. Fractions < 1 mm were used except for 5 samples that were subsampled before size-fractionation (samples #1, 5, 13 of the 1000 m trap and samples #5, 11 of the 3000 m trap of the first year deployment). Supernatant seawater was removed from the vials and the residues were then freeze-dried. Samples treated with formalin were rinsed with Milli-Q water three times before freeze-drying to remove formaldehyde. $\Delta^{14}C$ values of the formalin-treated samples did not exhibit any noticeably spurious behavior (supporting information Figure S1). Influence of formalin as a preservative on carbon isotope values were argued to be negligible [*Honda et al*., 2000, and references therein]. Dried aliquots of samples selected for carbon isotopic analysis were spread on petri-dishes and exposed to concentrated HCl vapor in a desiccator for ~12 h at room temperature to remove inorganic carbon [*Hedges and Stern*, 1984; *Komada et al*., 2008]. Each HCl-fumed sample was packed in doubled quartz tubes with CuO and silver wires, evacuated on a vacuum line, flame-sealed, then combusted at 850°C for 5 h. Produced CO_2 gas was cryogenically purified on a vacuum line. Both stable- and radio-carbon isotope ratios were measured at the National Ocean Sciences Accelerator Mass Spectrometry facility at WHOI [*McNichol et al*., 1994]. Three duplicate radiocarbon analyses yielded $\Delta^{14}C$ values that agreed within ±3 ‰. Empirical precision of $\Delta^{14}C$ measurement for sinking POC in our lab is smaller than ±10 ‰ based on multiple duplicate analyses. Precision of $\delta^{13}C$ measurements for sinking POC is better than 0.1 ‰.

Hydrographic data obtained by the Line W Project (available at http://www.whoi.edu/science/PO/linew/) [*Joyce et al*., 2005; *Peña-Molino et al*., 2012], especially the McLane Moored Profiler (MMP) and near-bottom current meter data at stations W5 (38.073°N and 68.667°W, water depth = 4110 m) were also used. For the time period relevant to our sediment trap deployments, the current data determined by an MMP at station W5 are available from July 2004 to June 2007 with a hiatus of about 1.5 years from December 2004 to April 2006.

Chlorophyll-*a* concentration data were retrieved from NOAA website (http://las.pfeg.noaa.gov/oceanWatch/oceanwatch.php). 8 day composite chlorophyll-*a* concentration data at 6 locations slightly upstream from the mooring site [(39.5°N, 68.2°W), (40.0, 68.0), (40.0, 67.4), (40.5, 67.4), (40.0, 67.0), (40.5, 67.0); indicated as a box in Figure 1] were averaged. This region was chosen as the potential provenance of the biogenic particles intercepted by the traps based on the alkenone-derived temperature data [*Hwang et al*., 2014].

3. Results

3.1. Particle Flux and Composition

Particles > 1 mm accounted for a small fraction of the total particle flux (average = 5 ± 5%; supporting information Table S1). This > 1 mm fraction contains swimmers that are not considered as part of passive particle flux. Hence, we focus our discussion on the particulate matter within the < 1 mm fraction. The mass flux of particles < 1 mm was highly variable temporally, ranging from 36 to 550 $mgm^{-2}d^{-1}$ (Figure 2a). Oftentimes, peak values were considerably higher than the adjacent samples. The particle fluxes at three depths were not strongly coupled both in terms of temporal variation and magnitude. High values were mostly observed at 3000 m. Also the particle flux was more variable at 3000 m than at the other two trap depths. The particle fluxes at 2000 m and 3000 m were similar with the exception of the first year when the annual average particle flux at 1000 m (209 ± 94 $mgm^{-2}d^{-1}$) was higher than at 2000 m (165 ± 100 $mgm^{-2}d^{-1}$). Consequently, the particle flux did not exhibit a decreasing trend with increasing depth. The average particle flux (± temporal variability) was 163 ± 77, 163 ± 96, and 210 ± 93 $mgm^{-2}d^{-1}$, at 1000 m,

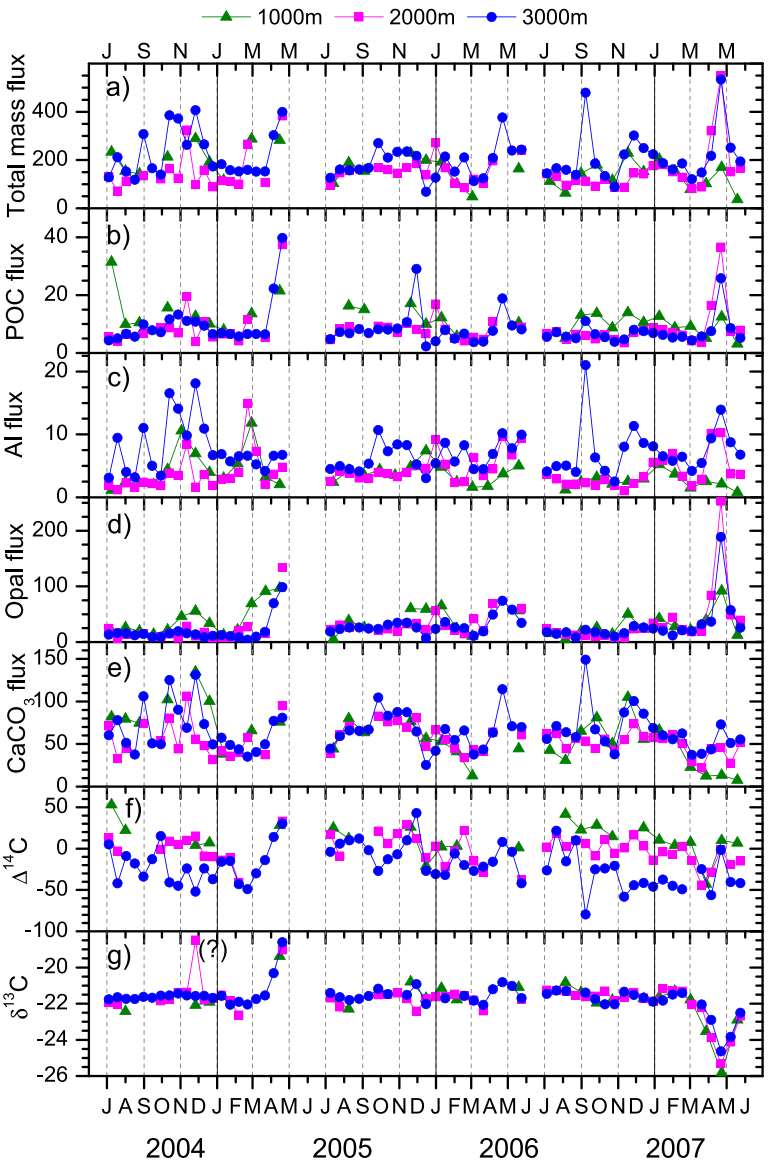

Figure 2. Fluxes (in $mgm^{-2}d^{-1}$) of (a–e) total mass, POC, Al, Opal, and $CaCO_3$, and (f and g) $\Delta^{14}C$ and $\delta^{13}C$ values of sinking POC in per mil.

2000 m, and 3000 m, respectively (Table 2; note that the reported variability about the average values reflects temporal variability within the time-series data, not measurement uncertainty).

In comparison with the total particle flux, POC flux at 1000 m was considerably higher than that at greater trap depths (Figure 2b). Only occasionally, POC flux at 2000 m and 3000 m was higher than that at 1000 m. In general, POC flux at 2000 m and 3000 m were more coherent in terms of both seasonal variation and magnitude. The average POC flux ($\pm$ temporal variability) was 11.5 ± 5.5, 8.5 ± 6.4, and 8.5 ± 6.2 $mgCm^{-2}d^{-1}$ at 1000 m, 2000 m, and 3000 m, respectively (Table 2). POC accounted for 2.5–13% (corresponding to 6.3–33% as organic matter) of sinking particles. The 1000 m trap showed the highest temporal variability in POC concentration (POC %). The average POC % deceased with increasing depth from 7.3 ± 2.0 at 1000 m to 5.3 ± 0.9 at 2000 m and 4.0 ± 1.6% at 3000 m (Table 2).

Al flux ranged from 1 to 21 $mgm^{-2}d^{-1}$, with high temporal variability (Figure 2c), and even the shallowest (1000 m) trap exhibited significant flux values. The Al flux was usually the highest at 3000 m. The only exceptions were in February, early March, and December 2005 and January 2006 when the flux at 2000 m was the highest. Each Al flux peak occurred as a pulse that lasted for only one sampling period, i.e., 14–16

Table 2. Values of Various Observed Parameters Averaged Over the 3 Years[a]

Parameters	Average Values ± Standard Deviation			Comparison of Magnitudes at Each Depth
	1000 m	2000 m	3000 m	
Particle flux (<1 mm)	163 ± 77	163 ± 96	210 ± 93	1000 m = 2000 m < 3000 m
POC flux	11.5 ± 5.5	8.5 ± 6.4	8.5 ± 6.2	1000 m > 2000 m = 3000 m
Al flux	3.7 ± 2.4	4.1 ± 2.7	7.3 ± 3.6	1000 m = 2000 m < 3000 m
Opal flux	35 ± 24	30 ± 37	26 ± 27	1000 m > 2000 m > 3000 m
Biogenic $CaCO_3$ flux	59 ± 30	55 ± 17	66 ± 24	1000 m = 2000 m < 3000 m
$C_{37:2}+C_{37:3}$ Alkenone flux[b]	3.2 ± 2.6	1.1 ± 1.1	0.78 ± 1.2	1000 m > 2000 m > 3000 m
Lithogenic flux	44 ± 28	50 ± 33	88 ± 44	1000 m < 2000 m < 3000 m
$\Delta^{14}C$ (‰)	+13 ± 20	−2 ± 17	−21 ± 24	1000 m > 2000 m > 3000 m
POC (%)	7.3 ± 2.0	5.3 ± 0.9	4.0 ± 1.6	1000 m > 2000 m > 3000 m
TN (%)	1.1 ± 0.3	0.7 ± 0.4	0.4 ± 0.2	1000 m > 2000 m > 3000 m
C/N	8.7 ± 0.7	9.7 ± 1.0	10.4 ± 1.1	1000 m < 2000 m = 3000 m
Biogenic opal (%)	21 ± 11	17 ± 9	12 ± 6	1000 m > 2000 m > 3000 m
Biogenic $CaCO_3$ (%)	36 ± 11	39 ± 11	33 ± 6	1000 m = 2000 m > 3000 m
Lithogenic material (%)	26 ± 9	32 ± 11	42 ± 8	1000 m < 2000 m < 3000 m

[a]The flux values are all in $mgm^{-2}d^{-1}$. The comparison is presented mainly as a guide in order to see the vertical trend. Instead of statistical analysis, we adopted 10% relative difference as criteria in comparison considering the uncertainties associated with measurements and conversions. For $\Delta^{14}C$ values, we adopted 10 ‰ as a criterion.
[b]From *Hwang et al*. [2014].

days. These pulses occurred throughout the sampling period and did not exhibit any clear seasonal trend. Interestingly, the results at 1000 m and 2000 m were coupled in both magnitude and temporal variability over most of the study period. However, when flux at 2000 m was high, such as in March–May 2006 and April–May 2007, the fluxes at 2000 m and 3000 m appear to be coupled. Average Al flux increased with increasing depth from 3.7 ± 2.4 at 1000 m to 4.1 ± 2.7 at 2000 m, and to 7.3 ± 3.6 $mgm^{-2}d^{-1}$ at 3000 m (Table 2).

In contrast to Al fluxes, the biogenic opal flux exhibited rather smooth temporal variability (Figure 2d). The flux at 1000 m exhibited bimodal seasonal variation with peaks in spring (April) and fall (November). In all 3 years, opal flux was highest in April. The flux at 1000 m was the highest with the exception of the peaks in April when the flux at 2000 m was the highest consistently every year. The average opal flux, 35 ± 24, 30 ± 37, and 26 ± 27 $mgm^{-2}d^{-1}$ at 1000 m, 2000 m, and 3000 m, respectively, decreased with increasing depth (Table 2).

The $CaCO_3$ flux exhibited high temporal variability (Figures 2e and 5). Although some data are absent, the 1000 m trap results showed that the flux was higher in fall/winter than in spring. Highest fluxes were observed at 3000 m (66 ± 24 $mgm^{-2}d^{-1}$ on average compared to 59 ± 30 and 55 ± 17 $mgm^{-2}d^{-1}$ at 1000 m and 2000 m, respectively). Temporal variability of $CaCO_3$ flux at 3000 m was similar to that of Al. In particular, coincident peaks were evident in $CaCO_3$ and Al fluxes. Average $CaCO_3$ flux was lowest at 2000 m (Table 2).

The sum of three biogenic (organic matter, $CaCO_3$, and opal) and lithogenic components accounted for almost all (99 ± 9%) of the sinking particle flux (supporting information Table S1). An exception was the two samples of the 2000 m trap for which the sum was 146 and 138%. For these two samples, Al and biogenic opal fluxes were higher than those of the 3000 m trap, and thus appear suspicious. However, we do not know the cause of this potential error at present. The contribution of particulate organic matter (POM) and opal decreased with increasing depth. In general, $CaCO_3$ accounted for the largest fraction of sinking particulate matter (31–36%), with the exception for the 3000 m trap where lithogenic component was the largest (~42%) (Figure 3 and Table 2). The average contribution of lithogenic material clearly increased with increasing depth from 27 ± 10 at 1000 m to 42 ± 8% at 3000 m.

3.2. Carbon Isotopic Composition

$\Delta^{14}C$ values of POC (< 1mm) ranged between +53 and −80 ‰ (Figure 2f), and were lower than the measured values for particulate organic matter collected in surface waters from this region (+58 ± 7 ‰, n=4) [*Hwang et al*., 2009a]. The $\Delta^{14}C$ values were highly variable temporally, with a difference between two consecutive samples of up to 90 ‰. The $\Delta^{14}C$ values did not show any clear seasonal trend. However, $\Delta^{14}C$ values at 3000 m in the second deployment period (–9 ± 20 ‰ on average) were slightly higher than the other two deployments (–21 ± 23 and −32 ± 24 ‰), although this difference was not statistically significant considering the large overall variability. Nevertheless, the higher $\Delta^{14}C$ values in the second deployment

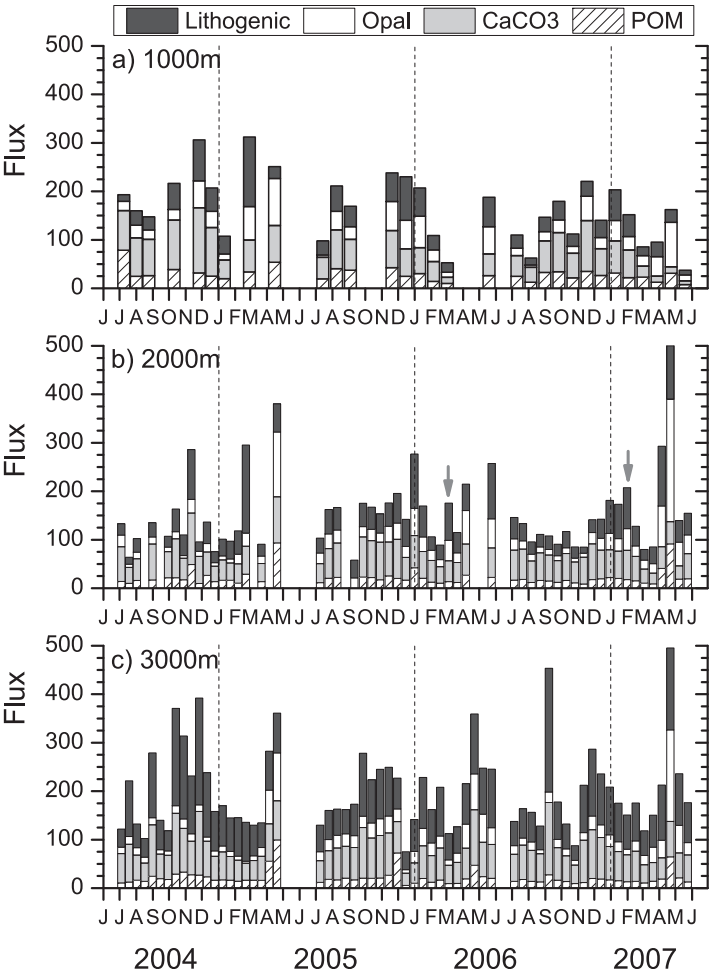

Figure 3. Fluxes (in $mgm^{-2}d^{-1}$) of POM, $CaCO_3$, opal, and lithogenic material of sinking particles. The two samples indicated by arrows in Figure 3b are those for which the sum of the four components was abnormally high (>130% of the measured total mass, see text).

period are consistent with the lower Al flux for this period (7.8 ± 4.8 $mgm^{-2}d^{-1}$ in the second year versus 6.6 ± 2.3 and 7.4 ± 4.1 in the first and third years, respectively). Again, however, this difference was not statistically significant considering the large variability.

The $\Delta^{14}C$ values at different depths did not appear tightly coupled and the values differed both in terms of temporal variability and magnitude. In a few rare cases, such as during the spring bloom periods and in late March 2007, the $\Delta^{14}C$ values at all depths were similar. However, in general there is a conspicuous vertical gradient in $\Delta^{14}C$. For a given sampling period, $\Delta^{14}C$ value was typically highest at 1000 m while $\Delta^{14}C$ values at 3000 m were, with few exceptions, the lowest. The mean $\Delta^{14}C$ values at 1000 m, 2000 m, and 3000 m were $+13 \pm 20$, -2 ± 17, and -21 ± 24 ‰, respectively (it should be noted that the mean value for the 1000 m trap may not be representative because of incomplete data coverage).

$\delta^{13}C$ values of POC fell within a narrow range, between -20.7 and -22.7 ‰, with the exception of two cases in April 2005 and April 2007 (Figure 2g). These anomalous values were observed at all sampling depths and appear to reflect an actual phenomenon. It is interesting to note that the anomalous $\delta^{13}C$ values in the spring bloom period in 2005 and 2007 showed opposite signals (positive and negative anomalies, respectively). There was no observable vertical gradient in $\delta^{13}C$ values.

4. Discussion

4.1. Sources of Sinking Particles: Pelagic Versus Benthic

Unlike open ocean sites in which particle fluxes are mainly controlled by pelagic processes, laterally transported and/or locally resuspended sediment particles appear to be another major source of particles in the study region [*Hwang et al*., 2009b]. We therefore attempt to interpret the concentration, flux and biogeochemical properties of each component of particulate matter (i.e., biogenic opal, $CaCO_3$, POC, and lithogenic particles) as a result of mixing between these two sources (i.e., primary production in the overlying water column and resuspended sediment). Terrestrial material, another potentially important source of particles on the continental margin, would be included in either of the two sources depending on the mode of transport to the study site.

As listed in Table 2, some parameters exhibit a decreasing concentration/flux trend with increasing depth whereas others exhibit the opposite trend, and still others exhibit no trend. In this context, properties that

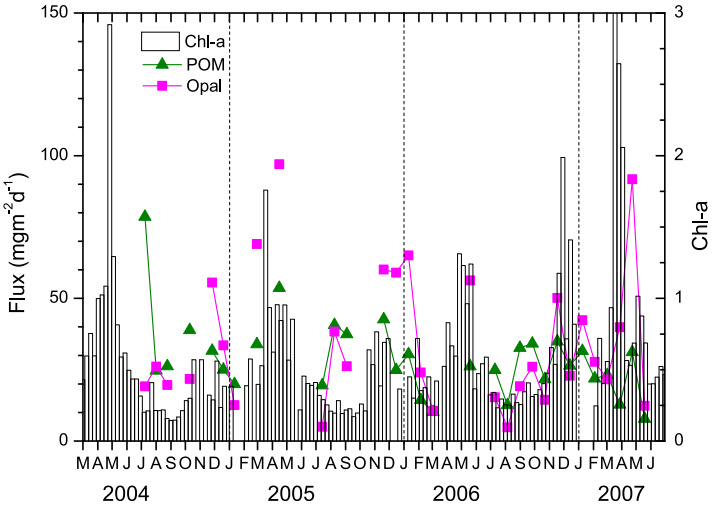

Figure 4. Opal and POM fluxes at 1000 m and satellite-derived chlorophyll-*a* concentration (data from NOAA, see text).

are influenced more by the pelagic source than the benthic source include the contents and fluxes of POC, TN, and opal, whereas the content and flux of $CaCO_3$ appears to be strongly influenced by benthic sources and the flux of Al is almost exclusively controlled by benthic supply.

A biannual cycle of biological productivity exists in the study region, evident from satellite-derived estimates of chlorophyll-*a* concentration: a larger spring bloom in March/April and a smaller fall bloom in around October/November [*Yoder et al.*, 2001]. In general, temporal variability of POC flux and biogenic opal flux at 1000 m reflected that of chlorophyll-*a* in surface waters (Figure 4). During the period of high biogenic opal flux especially from March to May in 2006 and 2007 (data in spring time do not exist for 2005; Figure 2), the $CaCO_3$ flux at 1000 m was low, implying that the spring blooms were caused by siliceous shell-forming organisms. $CaCO_3$ flux at 1000 m was high in fall and winter. This high $CaCO_3$ flux was positively correlated with the $C_{37:2}$ and $C_{37:3}$ alkenone flux (Figure 5, bottom; $R^2=0.266$, $P<0.005$, and $n=31$), suggesting that haptophyte production in surface waters was an important contributor to $CaCO_3$ flux at 1000 m.

High $CaCO_3$ flux values at 1000 m in late November and December 2004 coincided with low alkenone flux values, but with elevated Al fluxes, implying that these elevated $CaCO_3$ fluxes reflect sediment resuspension processes. This decoupling between the supply of resuspended $CaCO_3$ and alkenone flux is likely because surface sediment has much lower alkenone content than the sinking particles from the overlying surface water because of decomposition of alkenones during the vertical transit from production at the surface to the seafloor and subsequent degradation processes in the sediment mixed layer [*Hwang et al.*, 2014]. The

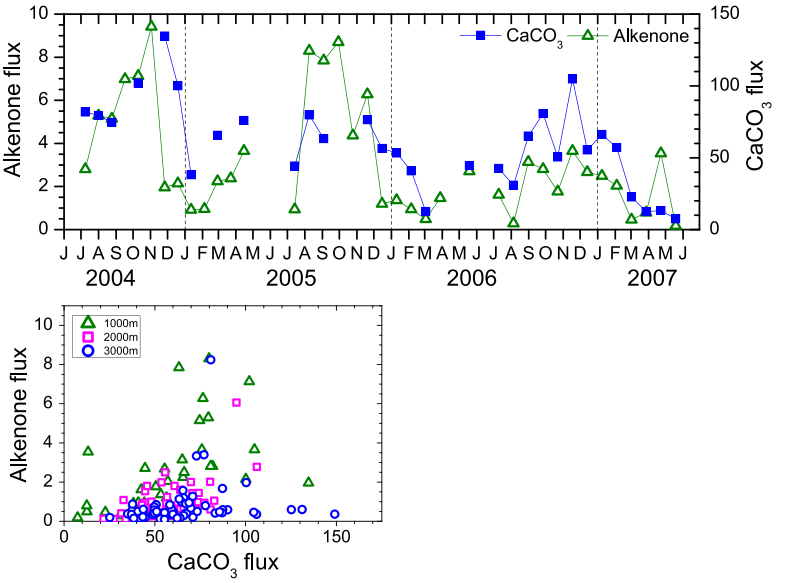

Figure 5. (top) The flux of $C_{37:2}$ and $C_{37:3}$ alkenones in $\mu gCm^{-2}d^{-1}$ and $CaCO_3$ in $mgm^{-2}d^{-1}$ at 1000 m trap depth and (bottom) alkenone fluxes versus $CaCO_3$ fluxes (same units) at three trap depths. The alkenone data are from *Hwang et al.* [2014].

vertical trend in $CaCO_3$ flux indicated increasing lateral supply of $CaCO_3$ from sediment resuspension. $CaCO_3$ concentration in surface sediments in this region was about 32% on average [*Seiter et al*., 2004]. $CaCO_3$ in sediments exists in various sizes from fine-grained detrital fragments to whole shells of foraminifera, coccolithophores, and other $CaCO_3$-producing organisms. Most of $CaCO_3$ in particles in the northwestern Atlantic was reported to exist as particles smaller than 63 μm [*Gardner et al*., 1985], facilitating its resuspension. *Lam et al*. [2015] reported that the majority ($\sim$79%) of particulate inorganic carbon resides in the small size fraction ($<$51 μm) of the suspended particles in the nepheloid layers along Line W. When resuspended, the dissolution rate of $CaCO_3$ is expected to be slow because the study site lies above the carbonate compensation depth. In contrast to the 1000 m samples, no correlation was found between the $CaCO_3$ flux and alkenone flux at 3000 m (Figure 5, bottom). With the exception of a few samples, alkenone flux was low ($<$ 2 $\mu gCm^{-2}d^{-1}$ as the sum of $C_{37:2}$ and $C_{37:3}$) regardless of the $CaCO_3$ flux. In comparison, the $CaCO_3$ flux at 3000 m exhibited a positive correlation with Al flux (Figure 8a), providing further evidence for a significant benthic source of $CaCO_3$.

Opal flux at 3000 m did not show a significant correlation with Al flux at the corresponding depth. Seawater is undersaturated with respect to opal dissolution, and therefore a large fraction of opal is dissolved in the water column and at the water-sediment interface [*DeMaster*, 2013]. Resuspension of opal from sediment to the water column will further enhance its dissolution because of its protracted exposure to low saturation levels. In addition, the opal content of surface sediments in this region is low ($<$5%) [*Seiter et al*., 2004]. Therefore, contribution of opal in resuspended particles is expected to be small.

4.2. Estimation of Contribution of Benthic Sources

Total particle flux was best correlated with the flux of lithogenic material, which accounted for the largest fraction of sinking particles when all data from all depths were considered (Figure 6). Pelagic input of Al from aeolian deposition was reportedly minor compared to sediment resuspension in this region [*Gardner et al*., 1985]. Annual dust deposition in this region was reported to be less than 1 $gm^{-2}yr^{-1}$, corresponding to 2.7 $mgm^{-2}d^{-1}$, based on a global eolian model [*Mahowald et al*., 2005]. This value corresponds to 0.22 $mgm^{-2}d^{-1}$ as Al flux, accounting for only $\sim$ 6%, 5%, and 3% of the average Al flux at 1000, 2000, and 3000 m, respectively. Hence, Al serves as an excellent proxy for resuspended sediment because lithogenic material represented by Al comprises a major fraction of these continental margin sediments [*Gardner et al*., 1985]. Lateral supply of lithogenic particles was therefore estimated simply from Al flux of sinking particles (Al flux$\times$12.15).

Radiocarbon can be used as a tracer for aged organic matter associated with resuspended sediment. $\Delta^{14}C$ values of sinking POC are expected to show a negative correlation with Al content in sinking particles [*Hwang et al*., 2010], which was clearly observed in this study (Figure 7). The y-intercept of the extrapolated trend line on the $\Delta^{14}C$-Al % plot (+51 $\pm$ 5 ‰, R^2=0.57, when a linear trend line was adopted, using all available 133 data points) should correspond to the $\Delta^{14}C$ value of the fresh POC end member, which is virtually identical to the observed $\Delta^{14}C$ values of POC collected in the surface water at or near the study site (58 $\pm$ 7 ‰, n=4) [*Hwang et al*., 2009a]. However, data points exhibit significant scatter on the $\Delta^{14}C$-Al % plot (R^2 of linear regression = 0.57; Figure 7). Potential causes of the scatter may include: (i) varying provenance of resuspended sediment exhibiting different $\Delta^{14}C$ values, (ii) inclusion of resuspended but fresh (higher $\Delta^{14}C$) POC that has not been consolidated within the mixed layer of surface sediments ("rebound POC") [*Lampitt et al*., 2000], and (iii) alteration of Al % due to nonuniform contributions of $CaCO_3$ and opal. The first hypothesis is plausible because there is a large gradient in $\Delta^{14}C$ of surface sediment across the continental margin: the $\Delta^{14}C$ values of the 0–1 cm sediment horizons at 23 locations in the

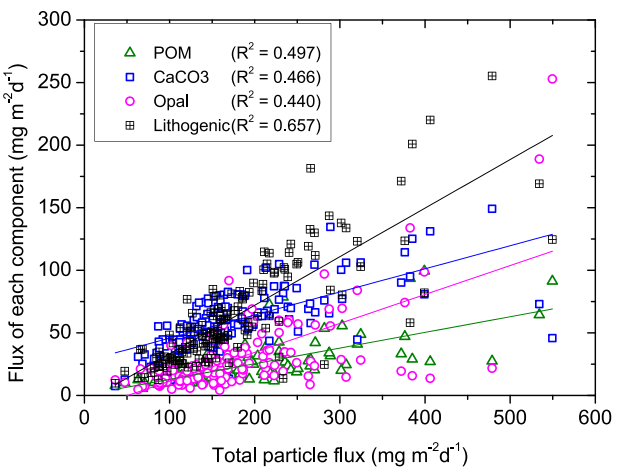

Figure 6. Fluxes of POM, opal, $CaCO_3$, and lithogenic material plotted versus total particle flux. P values of the regressions were $\ll$ 0.0001.

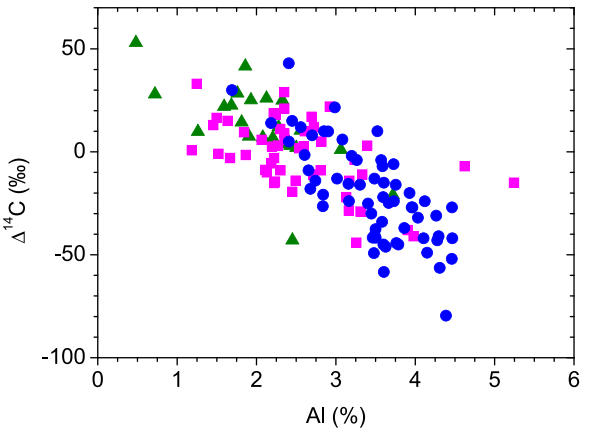

Figure 7. $\Delta^{14}C$ values of sinking POC versus aluminum concentration in sinking particles (green triangles = 1000 m, magenta squares = 2000 m, and blue circles = 3000 m).

northwest Atlantic margin (depth range between 281 and 3865 m) ranged between −93 and −338 ‰ with the average of −214 ± 60 ‰ [*Griffith et al.*, 2010, and also in supporting information Table S1). The 1000 m trap may be more influenced by resuspension and across-margin supply from adjacent shelf sediments, whereas the 3000 m trap from slope sediments that receive materials entrained along-margin by the DWBC. Further studies using other tracers such as Nd isotopes are necessary to constrain the provenance of resuspended sediment particles collected in the sediment traps.

To estimate organic matter contributions from benthic sources (resuspension), two scenarios were adopted: resuspension mainly derived from shelf sediment (depth = 100 m, $\Delta^{14}C = -140 \pm 50$ ‰) or from slope sediment (depth = 3000 m, $\Delta^{14}C = -260 \pm 50$ ‰). The $\Delta^{14}C$ values of surface sediments at depths of 100 m (shelf) and 3000 m (slope) were estimated based on the relationship between the water depths and the $\Delta^{14}C$ values of the above-described core-top sediment samples ($\Delta^{14}C$ in ‰ = −0.0411×depth in meters − 136). For fresh (pelagic) POC source, a $\Delta^{14}C$ value of +60 ± 20 ‰ was adopted. Based on radiocarbon mass balance using the shelf sediment $\Delta^{14}C$ (–140 ‰) as end member, contribution of POC from resuspended shelf sediment was estimated to be 26 ± 10, 31 ± 8, and 36 ± 12%, at 1000 m, 2000 m, and 3000 m, respectively, and the flux of fresh POC was estimated to be 9.3 ± 6.0, 6.0 ± 5.4, and 5.4 ± 5.5 $mgCm^{-2}d^{-1}$. If the slope sediment $\Delta^{14}C$ (–260 ‰) as end member was used, contributions of resuspended sediment to POC would be 18 ± 10, 20 ± 8, and 22 ± 12%, and the flux of fresh POC would be 9.4 ± 6.0, 6.8 ± 5.9, and 6.6 ± 5.7 $mgCm^{-2}d^{-1}$, at 1000 m, 2000 m, and 3000 m, respectively (see Figure 9). If "rebound POC" was indeed significant, then actual contributions from the benthic source would be larger than these estimates. The fresh POC flux estimated between 1000 and 3000 m from the above scenarios corresponded to 0.6∼0.9% of the average primary production, ∼980 $mgCm^{-2}d^{-1}$ at the study site (data were obtained from NOAA ERDDAP website, http://coastwatch.pfeg.noaa.gov/erddap/index.html).

Because the POC content of surface sediments is typically several-fold smaller than that of sinking particulate matter, overall contributions of resuspended sediment to sinking particulate load must be much higher than these estimates [*Kim et al.*, 2015]. The $CaCO_3$ flux showed a positive correlation with Al flux at 3000 m, implying that benthic sources of $CaCO_3$ were most prominent at this depth (Figure 8). We used the y-intercept on the plot of $CaCO_3$ flux versus Al flux, 26 $mgm^{-2}d^{-1}$, to infer an average $CaCO_3$ flux from the pelagic realm. This value corresponded to 39% of the total $CaCO_3$ flux at 3000 m on average, implying that the majority (61%) of $CaCO_3$ at this depth was supplied via sediment resuspension (Figure 9). The opal flux exhibited little or no correlation with the Al flux (Figure 8). The opal flux at 3000 m was among the lowest when Al flux was elevated (15 and 21 $mgm^{-2}d^{-1}$), suggesting that the biogenic opal content of resuspended particles was very small. Therefore, we assumed that the benthic source of opal was negligible. We estimate that benthic particle contributions, taken as the sum of fluxes of lithogenic material, $CaCO_3$ (observed flux − 26 $mgm^{-2}d^{-1}$), and aged organic matter, accounted for 67 ± 9% of the total flux at 3000 m (using either $\Delta^{14}C$ values, −140 or −260 ‰, as the resuspension end member would cause only a 1% difference).

It is more challenging to estimate the contribution of the benthic source to the $CaCO_3$ flux at 1000 m and 2000 m since at these trap depths the $CaCO_3$ flux and Al flux did not exhibit any clear correlation. We assumed that the ratio of $CaCO_3$ flux to lithogenic particle flux of the resuspended particles at 3000 m (40/88=0.45, see Figure 9) was also applicable at the upper two depths, and estimated the flux of laterally supplied $CaCO_3$ based on Al flux. As a validation, we compared the increase in $CaCO_3$ flux from 1000 m to 2000 m (indicative of lateral supply between the two depths) to the corresponding increase in Al flux for the last three samples at 1000 m and the last four samples at 2000 m (note that the sampling intervals at the two depths were different). The ratio of $CaCO_3$ flux increase over Al flux increase from 1000 m to

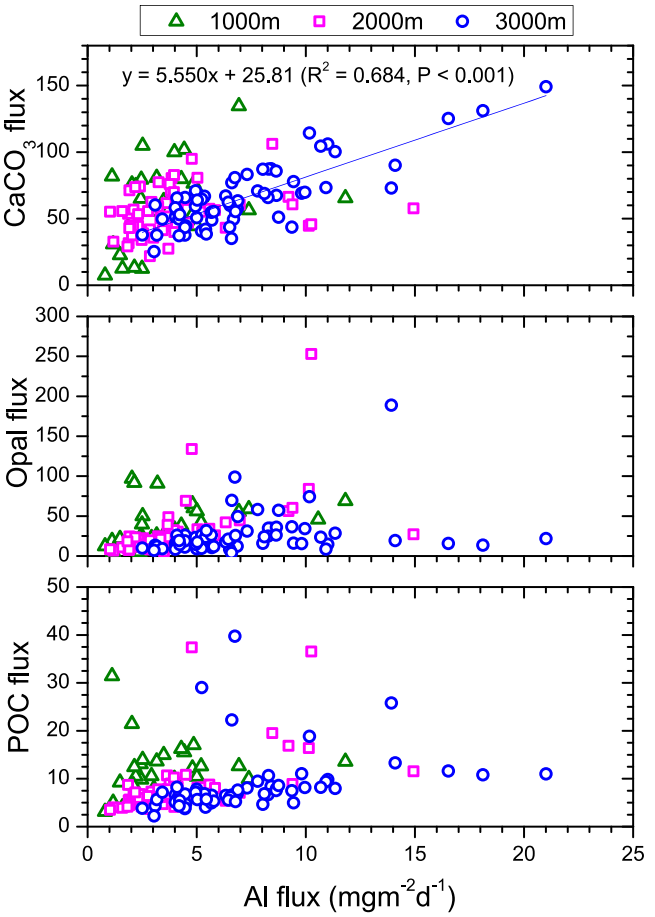

Figure 8. Fluxes (in $mgm^{-2}d^{-1}$) of (top) $CaCO_3$, (middle) opal, and (bottom) POC plotted versus aluminum flux. The linear trend line in the top panel is for the 3000 m samples.

2000 m was 0.31, [(84 − 42)/(275–138)=0.31], which was not drastically different from the ratio at 3000 m. $CaCO_3$ from benthic inputs, estimated from this ratio (0.45) and the lithogenic material flux, accounted for 33 and 39% of the observed $CaCO_3$ flux at 1000 m and 2000 m, respectively. Together, aged POM (based on slope sediment end member), $CaCO_3$, and lithogenic material from the benthic source accounted for 42 and 47% of total particle flux at 1000 m and 2000 m (Figure 9), implying that lateral supply of resuspended sediment was substantial even at these intermediate water depths.

Vertical variation in fluxes of each component is presented in Figure 9. Pelagic POC flux attenuated by about 30% from 1000 m to 3000 m. Lateral supply of POC at three depths was almost comparable and accounted for an increasing fraction of POC flux with increasing depth. Opal flux decreased by about 26% without significant lateral supply while $CaCO_3$ flux decreased by about 33%. However, $CaCO_3$ flux was counterbalanced by lateral supply considerably, and lithogenic particle flux approximately doubled from 1000 m to 3000 m. Overall, pelagic-sourced particle flux decreased from 98 to 69 $mgm^{-2}d^{-1}$ while this flux was counteracted by increased lateral particle flux from 69 to 133 $mgm^{-2}d^{-1}$. *Lam et al.* [2015] reported that opal accounted for the smallest fraction of suspended particles throughout the water column while lithogenic component accounted for increasing fraction with increasing depth. Lithogenic component accounted for over 70% of suspended particles (especially, 79% of small size fraction) in the benthic nepheloid layer at a nearby station (Station GT11–4). When compared to the composition of suspended particles, sinking particles contained higher concentrations of opal and lower concentrations of lithogenic material.

4.3. Hydrodynamic Control of Lateral Particle Inputs

Sinking particles during vertical transit are expected to move southwestward at the trap mooring site due to prevailing currents of DWBC [*Toole et al.*, 2011]. Each component of the southwestward flowing current (i.e., Upper Labrador Sea Water, Classical Labrador Sea Water, Iceland-Scotland Overflow Water, and Denmark-Strait Overflow Water [*Toole et al.*, 2011]) may entrain particles resuspended from the corresponding depths on the slope to form INLs and the BNL.

The Al fluxes at 1000 m and 2000 m were similar, but differed from that at 3000 m both in terms of magnitude and temporal variability. Together with other properties (Table 2), the vertical distribution of Al flux implies that the lateral supply of lithogenic particles may operate differently in the water column and near the seafloor. The 3000 m trap was within the BNL [*Hwang et al.*, 2009a], therefore it is expected to be affected by processes occurring in the BNL in addition to those in the overlying water column. During intervals such as March-May 2006, and January and April 2007, Al fluxes at 2000 m and 3000 m were similar with both markedly higher than those at 1000 m. This observation may imply that a cloud of high particle concentrations extended upward at least to 2000 m depth during these periods. The presence of INLs located

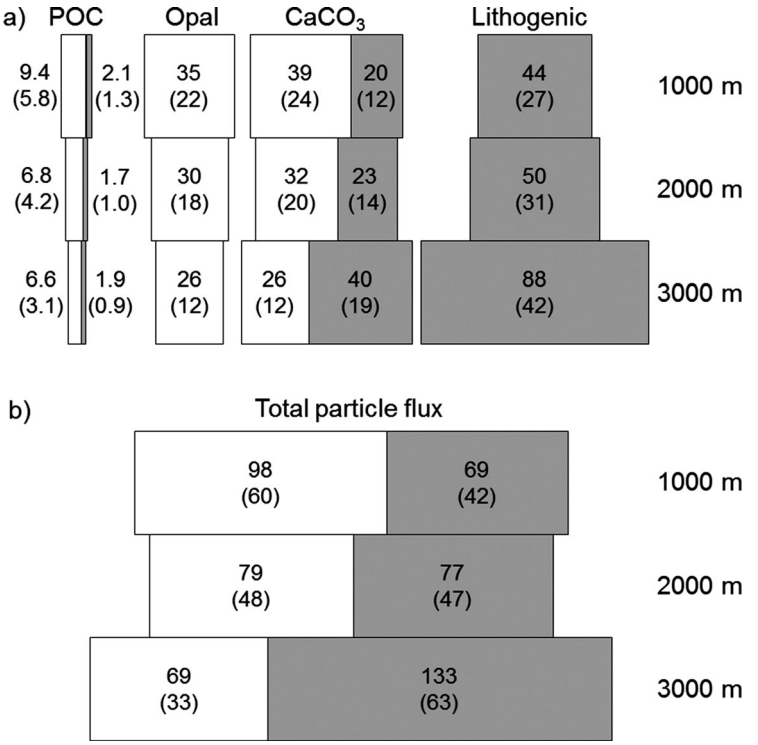

Figure 9. Fluxes in $mgm^{-2}d^{-1}$ of POC, opal, $CaCO_3$, lithogenic particles, and total particle flux at three depths, apportioned into pelagic (white) and benthic (shaded) sources. The values in the parentheses are per cent contributions of each component. The overall widths of the bars are proportional to the flux. Slight differences (< 5%) between the sum of the components and the determined total particle flux are derived from the error in conversion from element concentrations to each component.

between the 1000 m and 2000 m traps, thereby affecting only the 2000 m and 3000 m traps, represents an alternative explanation. The optical backscatter sensor data measured at 3000 m exhibited high particle concentration events in late August, October and late December 2005, with weaker signals (lower particle concentrations) thereafter (supporting information Figure S2). The signal did not exhibit any clear correlation with the Al flux either at 2000 m or 3000 m. Although the causes of this lack of correlation are not understood at the moment, different sensitivity of the optical backscatter sensor to small suspended particles and relatively large sinking particles may be a reason [*Bunt et al*., 1999].

In order to understand the controlling mechanisms of the sporadic supply of resuspended particles within the BNL, the Al flux variability at 3000 m was compared with deep current velocities obtained by an MMP and a current meter moored at station W5, approximately 160 km downstream from the sediment trap deployment site (38.073°N, 68.667°W; Figure 1). It is well known that resuspension of sediment is primarily linked with seabed shear stress induced by bottom currents [*Valipour et al*., 2017, and references therein]. Since no bottom current measurements were conducted at the trap mooring site, we used near-bottom current velocity data obtained from station W5 to draw comparisons with the Al flux variability by means of time-lagged cross correlation analysis. The raw data were filtered using the Butterworth low-pass filter with a half-power cutoff at 14 days after daily interpolation in order to quantify the correlation. Degree of freedom for this correlation was about 40. The near-bottom current velocity and Al flux showed the maximum correlation with the former leading the latter by 25–35 days (Figure 10c). The strong near-bottom current events were likely associated with bottom-intensified characteristics of deep currents. Vertical difference of current speeds at 3000 m and 3500 m ($\Delta U = U_{3500m} - U_{3000m}$, where U is current speed, as a proxy of sheer stress) obtained from the MMP exhibited similar variability to the near-bottom current variability. The bottom-intensified deep currents and Al flux also exhibited the maximum correlation, similar with the case of near-bottom current, at time lags of 25∼35 days.

The bottom-intensified flows are often regarded as footprints of topographic Rossby waves. The existence of topographic Rossby waves in this area with a period of a few weeks has been reported in several studies [*Thompson*, 1971; *Thompson and Luyten*, 1976; *Fratantoni and Pickart*, 2003; *Peña-Molino et al*., 2012], dominantly affecting near-bottom current variability. The correlation between the Al flux and the near-bottom current implies that local resuspension events at least partly caused by strengthening of the bottom-intensified deep current likely resulted in supply of sedimentary particles to the 3000 m trap. Alternatively, these properties may be a manifestation of high-current-speed events ("benthic storms" in *Hollister and McCave* [1984]). As *Gardner et al*. [1985] noted, horizontal advection and diffusion may be more important than local resuspension of sediments, and by inference in particle supply to the 3000 m trap. Comparison of

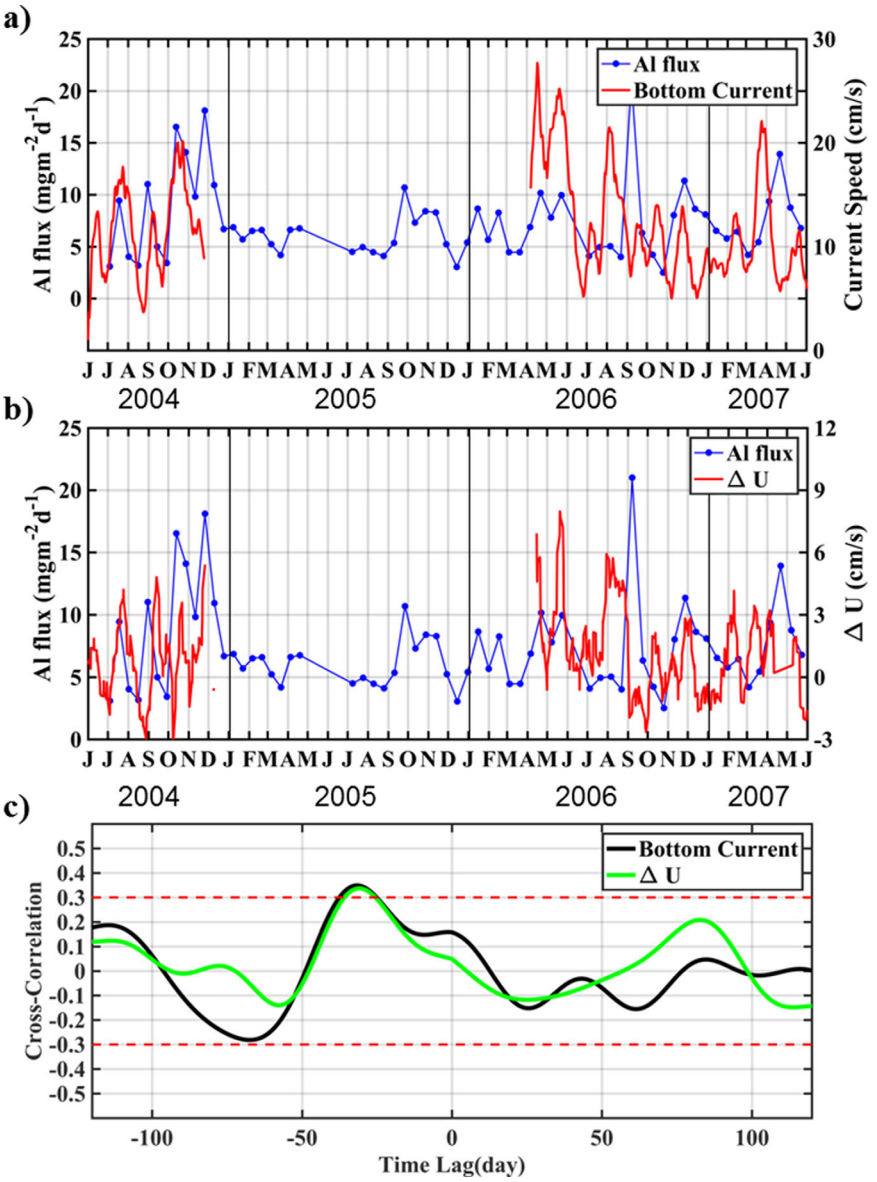

Figure 10. (a) Aluminum flux at 3000 m and near-bottom current speed at mooring station W5 (38.073°N and 68.667°W, water depth = 4110 m), (b) The Al flux and difference in current speed between 3000 m and 3500 m ($\Delta U = U_{3500m} - U_{3000m}$) at W5, (c) The lagged cross-correlations between the Al flux and the near-bottom current (black line) as well as between the Al flux and the vertical difference of the currents (green line). Dashed lines show statistical significance levels of 99%. Significance of > 99% was obtained with a time lag between 25 and 35 days, with the current variabilities leading the Al flux.

alkenone-temperatures between sinking particles at 3000 m and the underlying surface sediment also implied that lateral transport of POC from colder regions was occurring in addition to local resuspension [*Hwang et al*., 2014]. In contrast, the Al flux at 1000 m and 2000 m did not show any clear correlation with the horizontal current strength measured at the Line W mooring sites, again implying different controls of lateral particle supply in the water column.

Overall, our results imply that lateral particle supply can be a major source of sinking particles in continental margin settings, augmenting (and even dominating) vertical sinking of the biogenic particles from the overlying water column. Given the widespread influence of resuspended sediments on oceanic particulate organic carbon implied by radiocarbon contents of sinking POC [*Hwang et al*., 2010], this process should be incorporated in oceanic carbon cycle models. Quantitative assessment of the contribution of resuspended sediments to sinking particles in sediment trap studies will be critical to derive the global nature of this

phenomenon. In addition, the role of sediment resuspension in transformation of organic matter and other biogenic particles in the water column should be carefully examined.

5. Summary and Conclusions

We have examined various biogeochemical properties of sinking particles intercepted at three depths on a sediment trap mooring deployed at the 3000 m isobath on the New England slope in the Northwest Atlantic Ocean. A key research objective was to understand sinking particle fluxes in the context of physical forcing factors in the water column and biological productivity in surface waters of this dynamic region where the DWBC and the Gulf Stream interact.

We have found that each component of sinking particles had different dominant sources. For example at 50 m above the seafloor, opal flux was mainly dependent on vertical supply from biological production in overlying waters whereas $CaCO_3$ was mainly supplied by lateral transport of resuspended sediment. About 22–36% of sinking POC was estimated to derive from sediment resuspension depending on water column depth and choice of the end member $\Delta^{14}C$ value for the latter. While this ^{14}C mass balance approach and examination of correlations with Al flux sheds light on sediment resuspension as an important source of particulate matter to the water column, further geochemical investigations are necessary to establish the provenance of laterally supplied particles.

The availability of physical oceanographic data for the adjacent Line W transect proved to be useful in identifying mechanisms of sediment resuspension and particle supply within the BNL (3000 m sediment trap). However, factors controlling resuspended sediment delivery above the BNL at 1000 m and 2000 m, and coupling/de-coupling of Al flux between 1000 m, 2000 m and 3000 m traps during different time periods remain elusive. No clear correlation was found between the current velocity data of the Line W transect and the Al flux in the upper water column.

Approximately 42–47% of the total particle flux at 1000 m and 2000 m, respectively, was estimated to derive from sediment resuspension. This proportion increased to ~63% within the BNL, near the seafloor. Therefore, our understanding of the nature and fluxes associated with the biological pump will be prone to significant uncertainty without considering this secondary source of particles, particularly in locations that experience resuspension of sediment and subsequent lateral transport.

Acknowledgments

We thank F. Batista, L. Costello, A. Dickens, N. Drenzek, R. François, A. Gagnon, D. Griffith, L. Hmelo, J. Holtvoeth, M. Lardie, W. Martin, D. McCorkle, C. Payne, E. Roosen, J. Saenz, and M. Soon for participation in research cruises and for help with sampling. We also acknowledge help from the captains and crews on the *R/V Endeavor* and *R/V Oceanus*. We thank T. Joyce for the Line W data, staff at NOSAMS WHOI for carbon isotope measurements, and the WHOI Mooring Operations and Engineering Group for crucial assistance. We also thank the Editor and two anonymous reviewers for helping to improve the manuscript. This research was funded by the NSF Ocean Sciences Chemical Oceanography program (OCE-0425677; OCE-0851350) and by the Ocean and Climate Change Institute of WHOI. The data used are listed in the references and the supporting information Table S1 and a separate data set file. Hydrographic data of the Line W Project are available at http://www.whoi.edu/science/PO/linew/.

References

Bao R., C. McIntyre, M. Zhao, C. Zhu., S.-J. Kao, and T. I. Eglinton (2016), Widespread dispersal and aging of organic carbon in shallow marginal seas, *Geology*, *44*, 791–794, doi:10.1130/g37948.1.

Behrenfeld, M. J., and P. G. Falkowski (1997), Photosynthetic rates derived from satellite-based chlorophyll concentration, *Limno. Oceanogr.*, *42*, 1–20.

Bunt, J. A. C., P. Larcombe, and C. F. Jago (1999), Quantifying the response of optical backscatter devices and transmissometers to variations in suspended particulate matter, *Cont. Shelf Res.*, *19*, 1199–1220.

DeMaster, D. J. (2013), The diagenesis of biogenic silica: Chemical transformations occurring in the water column, seabed, and crust, in *Treatise on Geochemistry*, vol. 9, 2nd ed., pp. 103–111, Elsevier, Oxford, U. K.

Dennett, M. R., and S. J. Manganini (2006), PCR amplification of preserved ocean flux material, *Eos Trans. AGU*, *87*(36), Ocean Sci. Meet. Suppl., Abstract OS46D-09.

Dunne, J. P., J. L. Sarmiento, and A. Gnanadesikan (2007), A synthesis of global particle export from the surface ocean and cycling through the ocean interior and on the seafloor, *Global Biogeochem. Cycles*, *21*, GB4006, doi:10.1029/2006GB002907.

Fratantoni, P. S., and R. S. Pickart (2003), Variability of the shelf break jet in the Middle Atlantic Bight: Internally or externally forced?, *J. Geophys. Res.*, *108*(C5), 3166, doi:10.1029/2002JC001326.

Gardner, W. D., J. B. Southard, and C. D. Hollister (1985), Sedimentation, resuspension and chemistry of particles in the Northwest Atlantic, *Mar. Geol.*, *65*, 199–242.

Griffith, D. R., W. R. Martin, and T. I. Eglinton (2010), The radiocarbon age of organic carbon in marine surface sediments, *Geochim. Cosmochim. Acta*, *74*, 6788–6800.

Hedges, J. I., and J. H. Stern (1984), Carbon and nitrogen determinations of carbonate-containing solids, *Limnol. Oceanogr.*, *29*, 657–663.

Hedges, J. I. (1992), Global biogeochemical cycles: Progress and problems, *Mar. Chem.*, *39*, 67–93.

Hollister, C. D., and I. N. McCave (1984), Sedimentation under deep-sea storms, *Nature*, *309*, 220–225.

Hollister, C. D., and A. R. M. Nowell (1991), HEBBLE epilogue, *Mar. Geol.*, *99*, 445–460.

Honda, M. C., M. Kusakabe, S. Nakabayashi, and M. Katagiri (2000), Radiocarbon of sediment trap samples from the Okinawa trough: Lateral transport of ^{14}C-poor sediment from the continental slope, *Mar. Chem.*, *68*, 231–247.

Honjo, S., and K. W. Doherty (1988), Large aperture time-series sediment traps; design objectives, construction and application, *Deep Sea Res., Part A*, *35*, 133–149.

Honjo, S., J. Dymond, R. Collier, and S. J. Manganini (1995), Export production of particles to the interior of the equatorial Pacific Ocean during the 1992 EqPac experiment, *Deep Sea Res., Part II*, *42*, 831–870.

Honjo, S., S. J. Manganini, R. A. Krishfield, and R. Francois (2008), Particulate organic carbon fluxes to the ocean interior and factors controlling the biological pump: A synthesis of global sediment trap programs since 1983, *Prog. Oceanogr.*, *76*, 217–285.
Hwang, J., D. Montlucon, and T. I. Eglinton (2009a), Molecular and isotopic constraints on the sources of suspended particulate organic carbon on the northwestern Atlantic margin, *Deep Sea Res., Part I*, *56*, 1284–1297.
Hwang, J., S. J. Manganini, D. B. Montlucon, and T. I. Eglinton (2009b), Dynamics of particle export on the Northwest Atlantic margin, *Deep Sea Res., Part I*, *56*, 1792–1803.
Hwang, J., E. R. M. Druffel, and T. I. Eglinton (2010), Widespread influence of resuspended sediments on oceanic particulate organic carbon: Insights from radiocarbon and aluminum contents in sinking particles, *Global Biogeochem. Cycles*, *24*, GB4016, doi:10.1029/2010GB003802.
Hwang, J., M. Kim, J. Park, S. J. Manganini, D. B. Montlucon, and T. I. Eglinton (2014), Alkenones as tracers of surface ocean temperature and biological pump processes on the Northwest Atlantic margin, *Deep Sea Res., Part I*, *83*, 115–123.
Inthorn, M., T. Wagner, G. Scheeder, and M. Zabel (2006), Lateral transport controls distribution, quality, and burial of organic matter along continental slopes in high-productivity areas, *Geology*, *34*, 205–208.
Joyce, T. M., J. Dunworth-Baker, R. S. Pickart, D. Torres, and S. Waterman (2005), On the Deep Western Boundary Current south of Cape Cod, *Deep Sea Res., Part II*, *52*, 615–625.
Karakas, G., N. Nowald, M. Blaas, P. Marchesiello, S. Frickenhaus, and R. Schlitzer (2006), High-resolution modeling of sediment erosion and particle transport across the northwest African shelf, *J. Geophys. Res.*, *111*, C06025, doi:10.1029/2005JC003296.
Keil, R. G., and J. I. Hedges (1993), Sorption of organic matter to mineral surfaces and the preservation of organic matter in coastal marine sediments, *Chem. Geol.*, *107*, 385–388.
Kim, H. J., D. Kim, K. Hyeong, J. Hwang, C. M. Yoo, D. J. Ham, and I. Seo (2015), Evaluation of resuspended sediments to sinking particles by benthic disturbance in the Clarion-Clipperton nodule fields, *Mar. Georesour. Geotechnol.*, *33*, 160–166.
Komada, T., M. R. Anderson, and C. L. Dorfmeier (2008), Carbonate removal from coastal sediments for the determination of organic carbon and its isotopic signatures, $\delta^{13}C$ and $\Delta^{14}C$: Comparison of fumigation and direct acidification by hydrochloric acid, *Limnol. Oceanogr.: Methods*, *6*, 254–262.
Lam, P. J., D. C. Ohnemus, and M. E. Auro (2015), Size-fractionated major particle composition and concentrations from the US GEOTRACES North Atlantic Zonal Transect, *Deep Sea Res., Part II*, *116*, 303–320.
Lampitt, R. S., P. P. Newton, T. D. Jickells, J. Thomson, and P. King (2000), Near-bottom particle flux in the abyssal northeast Atlantic, *Deep Sea Res., Part II*, *47*, 2051–2171.
Mahowald, N. M., A. R. Baker, G. Bergametti, N. Brooks, R. B. Duce, T. D. Jickells, N. Kubilay, J. M. Prospero, and I. Tegen (2005), Atmospheric global dust cycle and iron inputs to the ocean, *Global Biogeochem. Cycles*, *19*, GB4025, doi:10.1029/2004GB002402.
Mayer, L. (1994), Surface area control of organic carbon accumulation in continental shelf sediments, *Geochim. Cosmochim. Acta*, *58*, 1271–1284.
McCave, I. N., and I. R. Hall (2006), Size sorting in marine muds: Processes, pitfalls, and prospects for paleoflow-speed proxies, *Geochem. Geophys. Geosyst.*, *7*, Q10N05, doi:10.1029/2006GC001284.
McCave, I. N., I. R. Hall, A. N. Antia, L. Chou, F. Dehairs, R. S. Lampitt, L. Thomsen, T. C. E. van Weering, and R. Wollast (2001), Distribution, composition and flux of particulate material over the European margin at 47°-50°N, *Deep Sea Res., Part II*, *48*, 3107–3139.
McNichol, A. P., E. A. Osborne, A. R. Gagnon, B. Fry, and G. A. Jones (1994), TIC, TOC, DIC, DOC, PIC, POC-unique aspects in the preparation of oceanographic samples for ^{14}C-AMS, *Nucl. Instrum. Methods Phys. Res., Sect. B*, *92*, 162–165.
Muller-Karger, F. E., R. Varela, R. Thunell, R. Luerssen, C. Hu, and J. J. Walsh (2005), The importance of continental margins in the global carbon cycle, *Geophys. Res. Lett.*, *32*, L01602, doi:10.1029/2004GL021346.
Peña-Molino, B., T. M. Joyce, and J. M. Toole (2012), Variability in the Deep Western Boundary Current: Local versus remote forcing, *J. Geophys. Res.*, *117*, C12022, doi:10.1029/2012JC008369.
Pickart, R. S. (2000), Bottom boundary layer structure and detachment in the shelfbreak jet of the Middle Atlantic Bight, *J. Phys. Oceanogr.*, *30*, 2668–2686.
Pusceddu, A., A. Gremare, K. Escoubeyrou, J. M. Amouroux, C. Fiordelmondo, and R. Danovaro (2005), Impact of natural (storm) and anthropogenic (trawling) sediment resuspension on particulate organic matter in coastal environments, *Cont. Shelf Res.*, *25*, 2506–2520.
Seiter, K. C. Hensen, J. Schroter, and M. Zabel (2004), Organic carbon content in surface sediments-defining regional provinces, *Deep Sea Res., Part I*, *51*, 2001–2026.
Taylor, S. R. (1964), Abundance of chemical elements in the continental crust: A new table, *Geochim. Cosmochim. Acta*, *28*, 1273–1285.
Taylor, S. R., and S. M. McLennan (1985), *The Continental Crusts: Its Composition and Evolution*, Blackwell Sci., Oxford, U. K.
Thompson, R. (1971), Topographic Rossby waves at a site north of the Gulf Stream, *Deep Sea Res. Oceanogr. Abstr.*, *18*, 1–19.
Thompson, R., and J. R. Luyten (1976), Evidence for bottom-trapped topographic Rossby waves from single moorings, *Deep Sea Res. Oceanogr. Abstr.*, *23*, 629–635.
Thunell, R., C. Benitez-Nelson, R. Varela, Y. Astor, and F. Muller-Karger (2007), Particulate organic carbon fluxes along upwelling-dominated continental margins: Rates and mechanisms, *Global Biogeochem. Cycles*, *21*, GB1022, doi:10.1029/2006GB002793.
Thunell, R. C. (1998), Seasonal and annual variability in particle fluxes in the Gulf of California: A response to climate forcing, *Deep Sea Res., Part I*, *45*, 2059–2083.
Toole, J. M., R. G. Curry, T. M. Joyce, M. McCarthy, and B. Peña-Molino (2011), Transport of the North Atlantic Deep Western Boundary Current about 39°N, 70°W: 2004–2008, *Deep Sea Res., Part II*, *58*, 1768–1780.
Turner, J. T. (2015), Zooplankton fecal pellets, marine snow, phytodetritus and the ocean's biological pump, *Prog. Oceanogr.*, *130*, 205–248.
Valdes, S. T., S. C. Painter, A. P. Martin, R. Sanders, and J. Felden (2014), Data compilation of fluxes of sedimenting material from sediment traps in the Atlantic Ocean, *Earth Syst. Sci. Data*, *6*, 123–145.
Valipour, R., L. Boegman, D. Bouffard, and Y. R. Rao (2017), Sediment resuspension mechanisms and their contributions to high-turbidity events in a large lake, *Limol. Oceanogr. Methods*, *62*, 1045–1065, doi:10.1002/lno.10485.
Yoder, J. A., J. E. O'Reilly, A. H. Barnarda, T. S. Moore, and C. M. Ruhsam (2001), Variability in coastal zone color scanner (CZCS) Chlorophyll imagery of ocean margin waters off the US East Coast, *Cont. Shelf Res.*, *21*, 1191–1218.